Finite size effects on the moment and ordering temperature in antiferromagnetic CoO layers

Y. J. Tang,[1,2,*] David J. Smith,[3] B. L. Zink,[1] F. Hellman,[1,2] and A. E. Berkowitz[1,2]
[1]*Physics Department, University of California, San Diego, La Jolla, California 92093*
[2]*Center for Magnetic Recording Research, University of California, San Diego, La Jolla, California 92093*
[3]*Department of Physics and Astronomy and Center for Solid State Science, Arizona State University, Tempe, Arizona 85287*
(Received 21 July 2002; published 7 February 2003)

The relationship between magnetic properties and microstructure of thin antiferromagnetic CoO layers in $\{CoO(X)/SiO_2(50\ \text{Å})\}_{25}$ multilayers has been investigated. The temperature decay of the thermoremanent moment, zero-field-cooled/field-cooled magnetization measurements, and specific heat were evaluated as indicators of the magnetic ordering temperature. The temperatures associated with each decreased slightly with decreasing CoO layer thickness from 100 to 30 Å, but then exhibited a sharp decrease for CoO layer thickness below 20 Å. This decrease has been previously observed, and was attributed to intrinsic finite size effects associated with broken magnetic bonds at the surfaces. In the present investigation, it was determined that the CoO layer was amorphous in these thinner layers, accounting for the dramatic drop in Néel temperature. For thicker CoO layers, all measures of magnetic ordering coincide, indicating a true Neel temperature, whereas they do not for the thinner films. The structural change of CoO from crystalline to amorphous also causes a significant change in the temperature dependence of the magnetization, due to an increased number of weakly coupled uncompensated spins.

DOI: 10.1103/PhysRevB.67.054408 PACS number(s): 75.70.−i, 75.40.−s, 68.55.−a, 68.37.−d

I. INTRODUCTION

Finite-size effects refer to deviations from bulk properties as sample dimensions are reduced. An intrinsic effect occurs in material systems for which one or more sample dimensions (e.g., the thickness of a layer or diameter of a particle) is comparable to the intrinsic length scale of the property being considered. One can also consider a ''surface-driven'' finite size effect due to a competition between the properties of atoms in the core of a particle or layer and at its surface, usually originating from the reduced magnetic coordination number or surface roughness. As an example, surface spins often possess a higher magnetic anisotropy than core spins, due to their reduced symmetry. In addition, chemical or structural effects may arise in small particles and layers, due to phenomena such as surface segregation, relaxation, or interface effects which can dramatically alter the properties of surface atoms beyond that due to reduced magnetic coordination number. These possible structural effects are often overlooked, in part because the small particle size makes structural characterization challenging.

As initially noted by Néel, small antiferromagnetic (AF) particles or thin AF layers may possess a moment due to inexact compensation of the magnetic sublattices, an effect which increases with decreasing AF particle size or layer thickness.[1] The properties of these uncompensated spins usually dominate the net magnetic properties of AF films or small particles, and their presence simultaneously facilitates and complicates a magnetic characterization. For thin AF films, the uncompensated spins arise primarily from the lower coordination of surface atoms, but may also include loosely coupled spins, e.g., between grains. When these uncompensated spins are tightly coupled to the magnetic spins of the AF core, they serve as a measure of the magnetic order of the core, including the direction of its Néel vector, and hence provide a measure of the Néel temperature T_N. However, when they are loosely coupled, they may dominate the magnetic measurements without providing information about the core magnetic order. Specific heat and neutron scattering measurements provide a valuable complement to magnetic measurements, since these measure an average properties of all the spins.

For monoxide AF thin films and fine particles, a variety of magnetic finite size effects have been observed.[2–13] These include suppression of the AF ordering temperature T_N and blocking temperature T_B, thermally induced fluctuations of the Néel vector, increased numbers of AF sublattices, time-dependent magnetization in high fields, and anomalous hysteresis behavior. The suppression of T_N or T_B has generally been described in terms of scaling theory, implying intrinsic finite size effects; these show a power law dependence on size or layer thickness, but the details of the dependence (the prefactor of the scaling) vary widely, suggestive of structural effects playing a significant role. Furthermore, T_B is not a thermodynamic transition, and is dependent on details of interfaces; the distinction between T_N and T_B was experimentally demonstrated and discussed by Carey *et al.*[11] and van der Zaag *et al.*[12]

The dependence of T_N on layer thickness for two-dimensional layers of AF CoO has been previously investigated using two different systems and methods, with significantly different results (despite showing a similar thickness scaling exponent).[5,6] Specific heat measurements of CoO/MgO multilayer (ML) films showed a relatively small decrease (~20 K) of the Néel temperature on reduction of the CoO layer thickness from 100 to 16 Å.[5] In contrast, a sharp decrease (~200 K) was found over the same thickness range for a CoO/SiO_2 ML, where T_N was identified as the temperature of the peak in the dc magnetic susceptibility.[6] It was not clear if the large difference in T_N observed in these systems at smaller thicknesses was due to the difference in measurement technique or the microstructure of the CoO films. A

magnetization measurement such as susceptibility, is dominated by uncompensated surface spins, which may or may not be tightly coupled to, or reflect the magnetic state of, the AF core. The specific heat measures the sum of the entropy changes of all the spins and hence is dominated by core spins for any particle size where a core is well defined. The difference in microstructure is significant. CoO and MgO grow epitaxially on each other, leading to large columnar grains which extend through the entire ML and long structural coherence lengths. In contrast, SiO_2 is amorphous and hence the growth of CoO is structurally terminated at each layer. As a result, the grain size for CoO in the CoO/SiO_2 MLs would be expected to be small, whereas it is quite large (hundreds of Å) in the CoO/MgO MLs.

In this paper, we report an experimental investigation of the microstructural, magnetic, and thermodynamic properties of antiferromagnetic CoO in CoO/SiO_2 MLs with different CoO layer thicknesses. The goal was to compare finite size effects for CoO layers in systems with very different grain sizes in order to determine whether the observed effects (reduction in T_N and thermomagnetic properties of the uncompensated spins) were dominated by reduced thickness or grain size. However, we found that due to the complex growth mechanism of the different layers in CoO/SiO_2 MLs, the CoO microstructure changes from crystalline to amorphous for CoO layer thicknesses below about 20 Å. This structural change has a tremendous effect on the ordering temperatures in the CoO/SiO_2 MLs as well as on the magnetic behavior below T_N. We conclude that this microstructure is the principal origin of the previously observed differences between CoO/SiO_2 and CoO/MgO MLs. For thicker CoO layers in the CoO/SiO_2 MLs, we observed microcrystalline CoO, and small shifts in magnetic properties as functions of layer thickness, but these may also be influenced by structural disorder.

II. EXPERIMENTAL DETAILS

The $\{CoO(X)/SiO_2(50\ Å)\}_{25}$ MLs were made by magnetron sputtering onto Si(100) substrates and onto SiN-membrane-based microcalorimetry devices designed for thin film heat capacity measurements. CoO was reactively dc sputtered using a Co target in the presence of Ar and O_2 and SiO_2 was rf sputtered from a SiO_2 target in Ar. The total gas pressure was 2 mTorr during sputtering, with an Ar to O_2 flow rate ratio of 15. The sputtering rate was 0.4 Å/s for CoO and 0.3 Å/s for SiO_2, respectively. The CoO thickness X and SiO_2 thickness (50 Å) were controlled by sputtering time; all films have 25 $CoO(X)/SiO_2(50\ Å)$ bilayers. Low and high angle x-ray diffraction (XRD) and transmission electron microscopy (TEM) were used to characterize the samples. A JEOL 4000EX high-resolution electron microscope operated at 400 keV was used to observe the local microstructure. Samples were tilted to the [110] projection of the Si substrate so that the electron beam direction was perpendicular to the ML growth direction. Standard mechanical polishing and argon ion milling were used to prepare the TEM samples in this cross-sectional geometry. The magnetic properties were measured with a Quantum Design SQUID (superconducting quantum interference device) magnetometer. Specific heat measurements were made using the relaxation method with SiN membrane-based microcalorimeters capable of measuring thin films ($\sim$6 μg mass) from 77 K up to 540 K. Details of the microcalorimeters and specific heat measurement can be found elsewhere.[14]

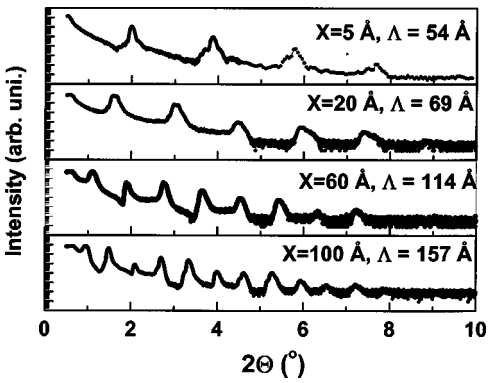

FIG. 1. Low angle XRD patterns for $\{CoO(X)/SiO_2(50\ Å)\}_{25}$ MLs. Superstructure lengths Λ for each sample are shown.

III. RESULTS

A. Microstructure

Typical low-angle XRD spectra for the MLs are presented in Fig. 1. The well-defined layered structure of the multilayers is evident from the large number of peaks in the XRD patterns seen for CoO thicknesses as small as 5 Å. The multilayer repeat distances (Λ) were calculated from the positions of the peaks and are listed in Fig. 1; these are in close agreement with the intended bilayer thicknesses.

Figure 2 shows high angle XRD patterns. Samples were tilted by several degrees during the measurement in order to reduce the strong intensity of the Si substrate (400) peak; the broad background peak from $2\theta = 75$ to 95° is due to residual scattering from this peak. For samples with CoO thickness $X \geqslant 20$ Å, polycrystalline CoO with a preferred

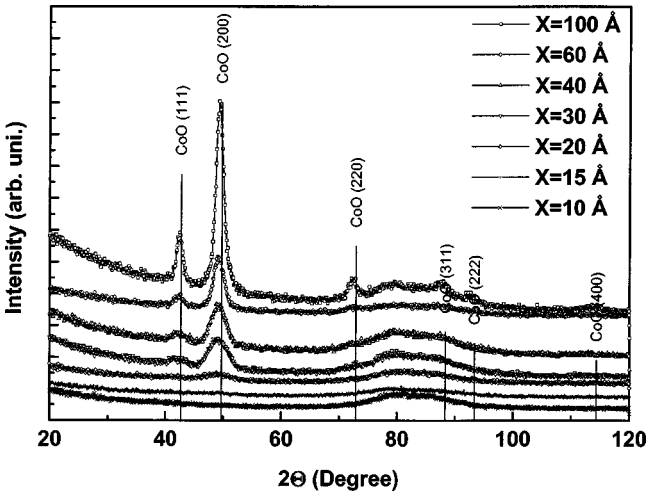

FIG. 2. High angle XRD patterns for $\{CoO(X)/SiO_2(50\ Å)\}_{25}$ MLs.

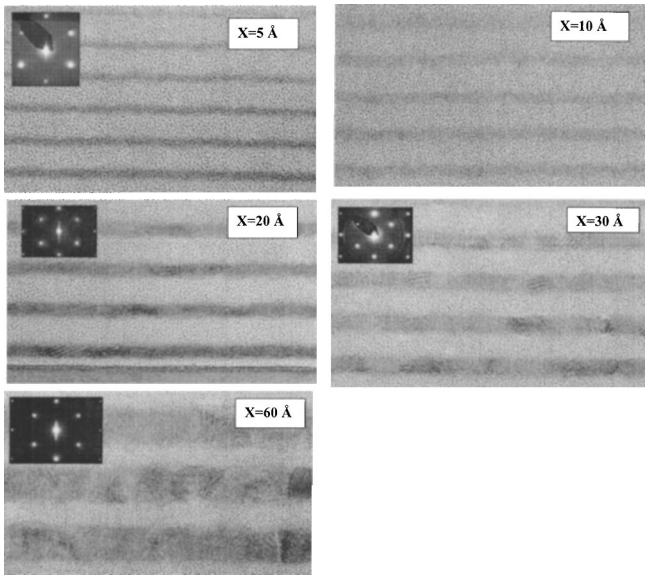

FIG. 3. Cross-section electron micrographs for $\{CoO(X)/SiO_2(50\ Å)\}_{25}$ MLs. Insets: electron diffraction patterns, showing numerous superlattice spots for the MLs.

(200) texturing is seen. Samples with CoO thickness smaller than 20 Å show no diffraction peaks. The average CoO grain size in the film normal direction was calculated from the full width half maximum of the (200) XRD peaks using the Scherrer equation.

Cross-section electron micrographs and diffraction patterns of several MLs are shown in Fig. 3. All samples show uniform layer thickness, with thicknesses in good agreement with the intended values. The diffraction patterns confirm the quality of the layering, with 5–20 superlattice spots visible on both sides of the central (000) diffraction spot; these superlattice spots are clearly visible even for the thinnest layers (5 Å). The superstructure lengths Λ were calculated from these spots for all samples, and are consistent with XRD results. The SiO_2 layers in all samples are uniformly amorphous. The CoO layers however show a crossover from good crystallinity for $X \geqslant 20$ Å to a uniformly amorphous microstructure for $X \leqslant 10$ Å. For the $X = 10-15$ Å samples, isolated crystalline grains are visible in the CoO layers, with the remainder of the layer amorphous.

Figure 4 shows a plot of grain size normal to the film determined from high angle XRD peak widths as a function of intended CoO thickness. The linearity and unity slope indicate that grain growth in the normal direction is terminated by the amorphous SiO_2 layers, consistent with the cross-section electron micrographs shown in Fig. 3. The average in-plane grain sizes were measured from the cross-section TEM images and are shown in Fig. 4 as a function of CoO layer thickness X. They increase with increasing X, approximately linearly, but as a weaker function of X than the grain sizes normal to the film, indicating a crossover in grain shape with X. For $X < 60$ Å, the in-plane grain size is larger than the normal direction grain size and the CoO layer thickness (flat platelets), while for $X \geqslant 60$ Å, the grain size normal to the film is larger than the size in-plane, consistent with the columnar CoO grains visible in the thicker MLs of Fig. 3.

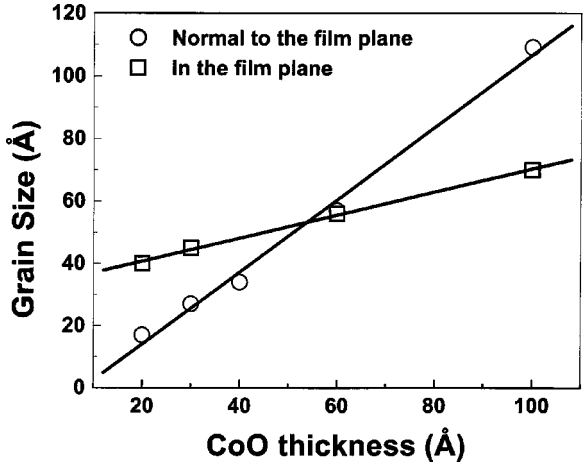

FIG. 4. Average grain size vs CoO layer thickness: in-plane (squares) from TEM images, normal to the film (circles) from TEM and XRD.

B. Magnetic ordering measurements

Three temperature-dependent measurements were used to investigate magnetic ordering in these samples: (a) the temperature and time decay of the thermoremanent moment (TRM) obtained by cooling in a field and then measuring on heating in zero field; (b) zero-field-cooled (ZFC) and field-cooled (FC) magnetization (both measured in 100 Oe); and (c) the specific heat (measured in zero field). When a field is applied to AF particles, the resulting moment is comprised of contributions from the uncompensated spins and from the AF susceptibility of those portions of the particles' cores which have bulk AF spin configurations.[15,16]

For the temperature decay of the TRM, samples were cooled from 330 to 10 K with an in-plane field of 25 kOe. The field was then set to zero, and the TRM was measured with increasing temperature in zero applied field; measurements take of order four minutes per temperature, and hence are relatively long time scale. The TRM is due to the presence of uncompensated spins whose moments are aligned by the applied field during cooling and which cannot relax to the equilibrium zero moment state due to exchange coupling to an antiferromagnetic core. It thus provides a direct measure of the blocking temperature of the grains. It will be dominated at higher temperatures by the largest grains in the CoO layers because the uncompensated spins in these larger grains are stabilized by a larger antiferromagnetic core. We call the temperature at which the TRM moment vanishes the maximum blocking temperature, $T_B^{\max}$. For $X < 20$ Å, both XRD and TEM results indicate that the CoO layers are amorphous, and thus it is possible that these materials will exhibit spin glass-type properties. In this case, we would interpret the vanishing of the TRM moment as a freezing temperature T_f. The large cooling field (25 kOe) was chosen for reasons of sensitivity; we have found that the magnitude of this cooling field has a small but measurable influence on the magnitude of the TRM moment but does *not* influence the temperature at which the TRM moment vanishes, i.e., at which thermal energy is sufficient to allow the moments to relax to the equilibrium $M = 0$ state.

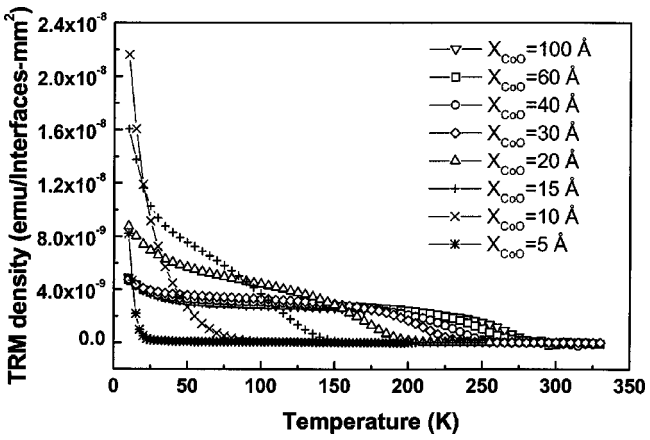

FIG. 5. Temperature dependence of the TRM moment for $\{CoO(X)/SiO_2(50\ Å)\}_{25}$ MLs. Samples were cooled to 10 K in a 25-kOe in-plane field; then the field was turned off and M measured on heating.

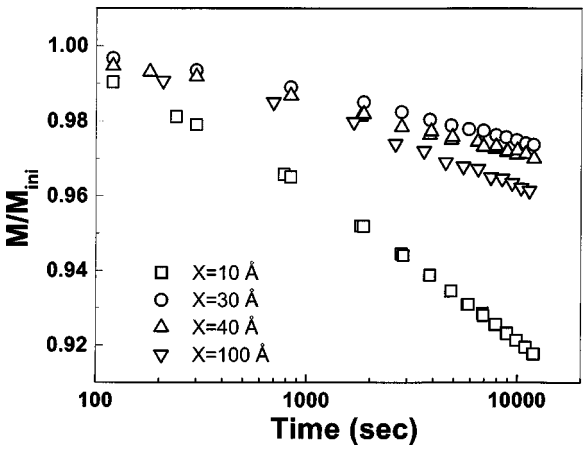

FIG. 6. Time relaxation of the TRM moment measured in zero field for $\{CoO(X)/SiO_2(50\ Å)\}_{25}$ MLs at 10 K. Cooling field 25 kOe.

The temperature dependence of the TRM is presented in Fig. 5 for various CoO layer thicknesses. Assuming that the TRM is dominated by interfacial uncompensated spins, at least in the crystalline samples with $X \geqslant 20$ Å, the TRM moment is shown in units of emu/interfaces-mm^2, the average moment per unit area of each interface layer. Since there are 50 interfaces in each sample (25 bilayers, each with two CoO interfaces), all data were normalized by the same constant. $T_B^{\max}$ decreases with decreasing CoO thickness down to 20 Å. A much stronger decrease of $T_B^{\max}$ occurs below 20 Å; this is the same thickness at which TEM started to show a crossover to an amorphous structure.

The temperature decay of TRM for samples with $X \geqslant 20$ Å generally exhibits two features: a ''plateau'' occurring over an intermediate temperature range from approximately 40 to 175 K where the TRM magnetization is roughly independent of the temperature, and a strong upswing at low temperature (<40 K). This behavior was seen previously in CoO/MgO superlattices and was ascribed to two kinds of uncompensated spin:[9–10] The ''plateau'' was associated with interfacial uncompensated spins that were strongly coupled to the AF cores, and the upswing at low temperature was associated with spins which were more weakly coupled to the AF core, possibly associated with spins in the grain boundaries. We note that as the CoO thickness decreases the ''plateau'' magnetization region moves to lower temperatures and gradually disappears. For samples with 5- and 10-Å-thick CoO layers, which TEM showed to be amorphous, there is no well defined AF core, hence no plateau, and a strong increase of TRM at low temperature is seen, associated with an increased number of weakly-coupled spins. The smaller TRM moment at low temperature for $X=5$ Å compared to $X=10$ Å is due to the decreased total CoO volume (the units in Fig. 5 are per interface not per unit volume), as well as the possibility of a ''frozen'' spin-glass state. For $X=15$ Å, the sample shows a transition behavior: a poorly defined ''plateau'' and a strong upswing, consistent with small amounts of crystallinity in an amorphous matrix.

We also measured the time dependence of the TRM moment at 10 K where the temperature decay exhibits the strong upswing for the thinner CoO layers. Figure 6 shows the normalized TRM moment vs time on a log scale for several samples. Decay times at 10 K for $X=30-100$ Å are similar, and are significantly longer than for $X=10$ Å consistent with the thinner samples increased number of weakly coupled spins.

We have also studied the temperature decay of the TRM moment for $\{CoO/SiO_2\}_n$ MLs with fixed CoO and SiO_2 thickness and varied number of bilayers n (from 5 to 80). The TRM moment per layer decrease with increasing n for the same CoO thickness in each layer. No significant structural variation through the film thickness for $n=25$ is seen in TEM images, but a more detailed structural study and a systematic study of the TRM moment behavior with increasing n would be needed to fully understand the TRM moment behavior. The maximum blocking temperature, $T_B^{\max}$ and the low temperature upturn is however, completely independent of n. We therefore conclude that any possible variations through the thickness of the 25 bilayer repeats for each sample are unimportant compared to the effects of changing the thickness of the individual layers.

Figure 7 presents ZFC/FC magnetization measurements, measured in 100 Oe with increasing temperature on samples cooled in 0/100 Oe respectively. There is an upswing of FC magnetization at low temperatures for all samples, similar to the TRM moment. A clear but broad peak is visible in the ZFC magnetization data for all X; the temperature of this peak decreases with decreasing X. For particles, this peak should be related to an *average* blocking temperature T_B^{ave}, associated with an average particle diameter. Figure 7 also shows a temperature T_{bif} at which the ZFC and FC magnetization curves bifurcate. T_{bif} is higher than T_B^{ave} and should be associated with the establishment of equilibrium for all spins. The data show that T_{bif} is equal to $T_B^{\max}$ found from the vanishing of the TRM in Fig. 6, consistent with it being interpreted as a temperature above which the spins are able to reach equilibrium. For $X=100$ Å, T_{bif} is the same as T_N, the bulk CoO ordering temperature; it decreases with de-

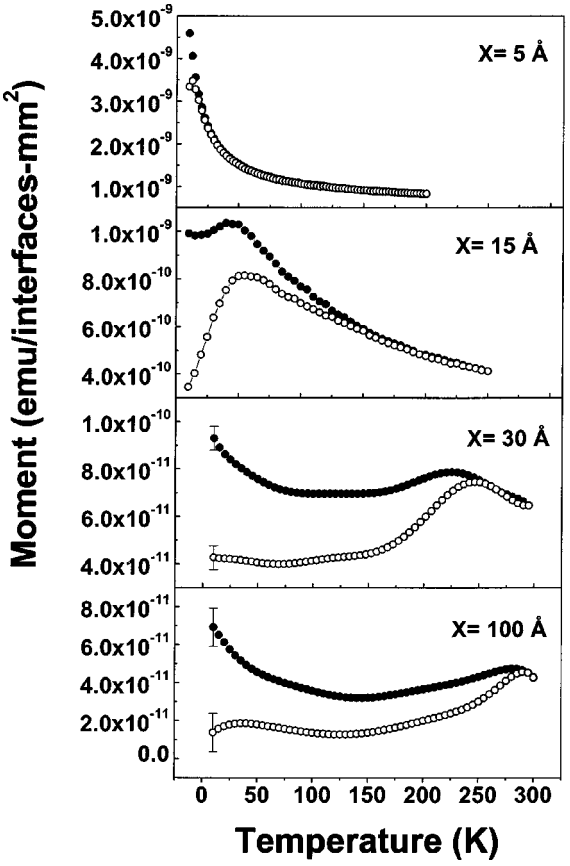

FIG. 7. ZFC/FC magnetization for $\{CoO(X)/SiO_2(50\ Å)\}_{25}$ MLs. Samples measured in 100 Oe.

creasing X, and the ZFC/FC curves have spin glass like characteristics for $X=5$ Å. For $X=10$, 15, and 20 Å, where the samples are substantially but not completely amorphous, $T_{\rm bif}=T_B^{\rm max}$ is significantly lower than the temperature of the peak in ZFC and FC magnetizations, $T_B^{\rm ave}$. For $X>20$ Å, $T_{\rm bif}=T_B^{\rm max}=T_B^{\rm ave}$, suggesting a reasonable uniformity of relaxation volumes, consistent with the more uniform grain size seen in TEM.

Figure 8 shows the specific heat C_p of CoO (in J/g K) for the CoO/SiO_2 MLs with different CoO thicknesses $X=20$, 40, 60, and 100 Å as well as for a single 3000-Å CoO layer. To obtain the data shown in Fig. 8, it was necessary to subtract contributions from the SiO_2 layers and from the calorimeter background (typically called the addenda in specific heat literature). The SiO_2 contribution was determined by measuring the specific heat of a 2500-Å-thick SiO_2 layer sputtered on a calorimeter device. The addenda include contributions from the SiN membrane, the thin film thermometers, leads, and heater, and a 2000-Å-thick Ag layer used to provide high internal thermal conductivity (necessary for the measurement). It was determined from measurements on a calorimeter device made in the same processing batch as the devices used for the MLs; previous work has shown a repeatability of better than 5% using this method.[14] The uncertainty of the sample C_p is dominated by the uncertainty in addenda C_p and was calculated based on the measured 3% variation

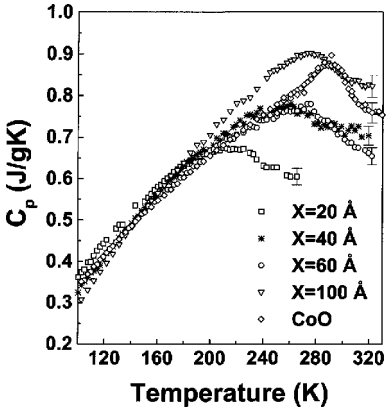

FIG. 8. Specific heat of CoO extracted from $\{CoO(X)/SiO_2(50\ Å)\}_{25}$ MLs with CoO thicknesses $X=20$, 40, 60, and 100 Å, and for a 3000-Å CoO layer. Representative error bars are shown at one T for each.

of the thermal conductivity, which should be the same for all devices from the same processing batch.

A peak in $C_p(T)$ represents the temperature of the maximum change in entropy from a paramagnetic to an antiferromagnetic state, i.e. the Néel temperature T_N for a homogeneous sample. For $X\geqslant 20$ Å, this peak should be interpreted as the Néel temperature of the *average* CoO grain because the magnetic entropy change associated with the ordering of the core spins is much larger than that associated with either their blocking ($k_B \ln 2$ per grain) or of any weakly coupled surface spins (surface spins are a small fraction of the total spins of even relatively small antiferromagnetic particles). For $X<20$ Å, where the TEM shows the CoO to be largely or entirely amorphous, a C_p peak would be interpreted as a freezing temperature, which is typically quite broad and at a temperature somewhat higher than the magnetically determined freezing temperature.

The C_p measurement shows $T_N=295$ K for the 3000-Å-thick CoO layer, in good agreement with published data. Even in this thick film, the peak, although relatively sharp, is broadened from the divergence or cusp expected for an ideal antiferromagnetic transition. This broadening is likely due to small inhomogeneities in composition and/or structure, but may also be associated with finite grain size (which limits the divergence of the coherence length) and spin frustration at the surfaces of these grains. As the CoO thickness in the MLs is reduced from 100 to 20 Å, the Néel temperature drops from 275 to 220 K and the peaks significantly broaden. For $X<20$ Å, no clear peak is seen; this is both because the signal from the very small amount of CoO in these films is small and because of the expected increased broadening of this peak in these amorphous layers. Their data are therefore not shown.

IV. DISCUSSION

Figure 9 summarizes the ordering and blocking temperatures measured from the TRM, ZFC/FC magnetization, and specific heat vs CoO thickness. We also show the Néel temperature of CoO in CoO/MgO superlattices determined from

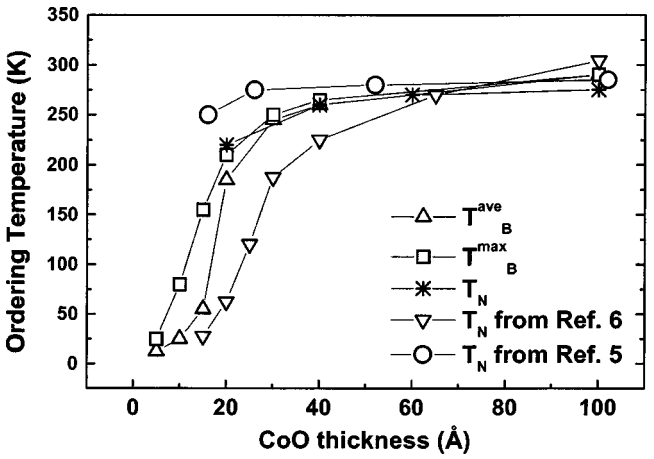

FIG. 9. Ordering temperatures T_B^{ave} (from peak in ZFC/FC magnetization), T_B^{max} (from ZFC/FC bifurcation T_{bif} and from vanishing of TRM), T_N (from specific heat peak) vs CoO layer thickness in $\{CoO(X)/SiO_2(50\ Å)\}_{25}$ MLs. Also shown are T_N for CoO/MgO MLs from specific heat from Ref. 5, and what was called T_N for CoO/SiO_2 MLs from the dc magnetic susceptibility peak from Ref. 6.

specific heat measurements,[5] and the Néel temperature of CoO/SiO_2 MLs shown in Ref. 6. All temperatures decrease with decreasing thickness, but with significantly different dependencies. For thicknesses greater than 20 Å, the Néel temperature obtained from the specific heat is very close to the blocking temperatures derived from TRM and FC/ZFC measurements, suggesting that these magnetic measurements accurately reflect magnetic ordering for these thicker layers.

At CoO thicknesses of 20 Å and below, the temperatures shown in Fig. 9 separate, a result we suggest is due to the increasing fraction of amorphous material. This is most noticeable at 10 and 15 Å where the peak in the susceptibility is nearly 100 °C lower than T_B^{max} obtained from the FC/ZFC bifurcation or the vanishing TRM moment. This large split in temperatures, together with the absence of a visible C_p peak, suggests that there is no true antiferromagnetic phase transition or long range ordering in these thinner samples. Even for the 20-Å sample, the C_p peak is at a temperature significantly higher than the other temperatures, indicating that the short range magnetic ordering which dominates C_p occurs at a higher temperature than the magnetic freezing seen by the magnetic measurements. Thus, even this 20-Å sample, which appears from TEM to be entirely crystalline with well-defined lattice planes visible in the micrographs, does not possess a well-defined magnetic ordering temperature which we should call T_N. We note that low angle x-ray scattering and TEM both show sharp superlattice peaks and clear compositional modulations for all these films, even for films with CoO thickness as thin as 5 Å where the CoO layer is amorphous. These superlattice peaks (as well as the TEM images) indicate that the interfaces remain sharp, with little or no interdiffusion and highly periodic multilayer structures even when both layers are amorphous. While these scattering techniques are relatively insensitive to oxygen, due to its low Z, both SiO_2 and CoO are stoichiometric compounds, and would not be expected to show oxygen interdiffusion. It is therefore highly likely that the significant changes seen in the magnetic properties of samples with thin CoO layers are directly related to the observed change from crystalline to amorphous, rather than to any possible interdiffusion.

Considering just the thicker samples where all temperature coincide and T_N is well defined, T_N for CoO in the present CoO/SiO_2 MLs is lower than that found for CoO in CoO/MgO superlattices for the same X (both from specific heat measurements). There are several possible reasons, all related to structural differences between the CoO layers in these two types of MLs. (1) Because the CoO is epitaxial to the MgO, there is a relatively large strain induced in the CoO in the CoO/MgO superlattice. (2) The in-plane grain size of CoO in CoO/MgO was found to be 250–500 Å, substantially larger than the CoO grain size in the CoO/SiO_2 MLs (3) The CoO in CoO/SiO_2 MLs is likely substantially more disordered than in CoO/MgO superlattices due to the necessarily disordered interfaces.

Finally, we note that the ordering temperature of CoO in CoO/SiO_2 MLs reported in Ref. 6 is significantly lower than what we obtained here for CoO thickness $X<60$ Å. Since no detailed structural information on the CoO was given in Ref. 6, we suggest that the ordering temperatures measured there from the dc magnetic susceptibility measurement is more likely to be the average blocking/freezing temperature of CoO grains rather than a true T_N. The films reported there may have been significantly structurally disordered or even amorphous for $X<40$ Å (the transition to the amorphous state which we found below ~20 Å is likely to depend on growth conditions).

In summary, we found that both grain size and the microstructure changes when the CoO layer thickness in $\{CoO(X)/SiO_2(50\ Å)\}_{25}$ MLs is reduced. For a CoO layer thickness less than 20 Å, the CoO is essentially amorphous. While the various temperatures associated with magnetic ordering and blocking (T_N, T_B^{max}, and T_B^{ave}) decrease slowly with decreasing CoO layer thickness from 100 to 20 Å, a sharp decrease is seen for thicknesses below 20 Å. We attribute this sharper decrease to the amorphous structure of the CoO in these layers, rather than an ''intrinsic'' finite size effect. The structural change from crystalline to amorphous also causes the disappearance of the ''plateau'' magnetization in the temperature decay of the TRM consistent with elimination of the core antiferromagnetic structure. Neutron scattering studies of the temperature dependence of the AFM Bragg elastic scattering peak could be used to confirm this vanishing of a well defined Néel vector in the thinner amorphous CoO films.[17]

ACKNOWLEDGMENTS

We thank M. F. Hansen and D. Kim for helpful discussions. This work was supported by DOE Grant Nos. DE-FG03-95ER45529 and DE-FG03-01ER15236. We acknowledge the use of facilities in the Center for High Resolution Electron Microscopy at Arizona State University.

*Email address: yjtang@ucsd.edu

[1] L. Néel, in *Low Temperature Physics*, edited by C. DeWitt, B. Dreyfus, and P. D. de Gennes (Gordon and Breach, New York, 1962).

[2] A. Punnoose, H. Magnone, and M. S. Seehra, and J. Bonevich, Phys. Rev. B **64**, 174420 (2001).

[3] R. H. Kodama and A. E. Berkowitz, Phys. Rev. B **59**, 6321 (1999).

[4] R. H. Kodama, Salah A. Makhlouf, and A. E. Berkowitz, Phys. Rev. Lett. **79**, 1393 (1997).

[5] N. Abarra, K. Takano, F. Hellman, and A. E. Berkowitz, Phys. Rev. Lett. **77**, 3451 (1996).

[6] T. Ambrose and C. L. Chien, Phys. Rev. Lett. **76**, 1743 (1996).

[7] E. E. Fullerton, K. T. Riggs, C. H. Sowers, S. D. Bader, and A. Berger, Phys. Rev. Lett. **75**, 330 (1995).

[8] S. S. P. Parkin and V. S. Speriosu, *in Magnetic Properties of Low-Dimensional Systems II. New Developments*, Proceedings of the Second Workshop, San Luis Potosi, Mexico, edited by L. M. Falicov, F. Mejia-Lira, and J. L. Moran-Lopez (Springer-Verlag, Berlin, 1990), pp. 110–120.

[9] K. Takano, R. H. Kodama, and A. E. Berkowitz, J. Appl. Phys. **83**, 6888 (1998).

[10] K. Takano, R. H. Kodama, and A. E. Berkowitz, Phys. Rev. Lett. **79**, 1130 (1997).

[11] M. J. Carey, A. E. Berkowitz, J. A. Borchers, and R. W. Erwin, Phys. Rev. B **47**, 9952 (1993).

[12] P. J. van der Zaag, Y. Ijiri, J. A. Borchers, L. F. Feiner, R. M. Wolf, J. M. Gaines, R. W. Erwin, and M. A. Verheijen, Phys. Rev. Lett. **84**, 6102 (2000).

[13] A. J. Devasahayam and M. H. Kryder, J. Appl. Phys. **85**, 5519 (1999).

[14] D. W. Denlinger, N. Abarra, Kimberly Allen, P. W. Rooney, M. T. Messer, S. K. Watson, and F. Hellman, Rev. Sci. Instrum. **65**, 946 (1994).

[15] J. T. Richardson, D. L. Yiagas, B. Turk, K. Forster, and M. V. Twigg, J. Appl. Phys. **70**, 6977 (1991).

[16] R. W. Chantrell, M. EI-Hilo, and K. O'Gray, IEEE Trans. Magn. **27**, 3570 (1991).

[17] J. A. Borchers, M. J. Carey, R. W. Erwin, C. F. Majkrzak, and A. E. Berkowitz, Phys. Rev. Lett. **70**, 1878 (1993).